

LHC as a photon-photon collider: bounds on $\Gamma_{X \rightarrow \gamma\gamma}$

S. I. Godunov¹, E. K. Karkaryan^{2,3}, V. A. Novikov¹, A. N. Rozanov^{2,4}, M. I. Vysotsky¹, and E. V. Zhemchugov¹

¹I.E. Tamm Department of Theoretical Physics, Lebedev Physical Institute, 119991, Moscow, Russia

²Institute for Theoretical and Experimental Physics, Moscow, 117218 Russia

³Moscow Institute of Physics and Technology (State University), Moscow, 141701 Russia

⁴Centre de Physique des Particules de Marseille, CPPM, Aix-Marseille Universite, CNRS/IN2P3, Marseille, France

December 10, 2020

Abstract

In the relatively recent CMS data, there is a hint on the existence of a resonance with the mass 28 GeV coupling to muons. Such a resonance should also couple to photons through the fermion loop, therefore it can be searched for in ultraperipheral collisions (UPC) of protons. We set an upper bound on the $X\gamma\gamma$ coupling constant from the data on $\mu^+\mu^-$ pair production in UPC at the LHC. Our approach can be used for similar resonances should they appear in the future.

1 Introduction

LHC designed as a proton-proton collider can also be considered as a photon-photon collider in which photons are produced in ultraperipheral collisions of protons. The interest in studying $\gamma\gamma$ collisions is twofold: first, QED processes like $\gamma\gamma \rightarrow l^+l^-$ [1–3], $\gamma\gamma \rightarrow W^+W^-$ [4–7], $\gamma\gamma \rightarrow \gamma\gamma$ [8–10] are investigated at very high energies never before accessible at particle accelerators and, second, production of new exotic particles can be looked for. The case of long-lived heavy charged particles was considered in [11]. Dark matter particles are discussed in [12–14]. In the paper [15] the production of exclusive $\gamma\gamma \rightarrow \mu^+\mu^-$ events in proton-proton collisions at a centre-of-mass energy of 13 TeV with the ATLAS detector was analyzed. The measurement was performed in the dimuon invariant mass interval $12 \text{ GeV} < m_{\mu^+\mu^-} < 70 \text{ GeV}$. If a resonance with the mass in this interval does exist and can decay to a $\mu^+\mu^-$ pair, we can obtain an upper bound on its coupling with two photons from the data provided in [15]. Evidence of such a resonance X with the mass (28.3 ± 0.4) GeV was reported by the CMS collaboration [16], and in what follows we will obtain bounds on its coupling to two photons. However being universal our approach can be used for another resonance if it exists.

As it was noticed in [17], X can be responsible for the deviation of the measured value of the muon anomalous magnetic moment a_μ from its theoretical value. Introducing the coupling Y of the scalar X to muons according to

$$\Delta\mathcal{L} = Y\bar{\mu}\mu X, \quad (1)$$

it was obtained in [17] that for $Y = 0.041 \pm 0.006$ one loop contribution $\delta a_\mu^X = (29 \pm 8) \times 10^{-10}$ explains the deviation of the measured value of a_μ from the Standard Model result. It was also shown that such couplings are consistent with other experimental bounds.

With this value of Y we get:

$$\Gamma_{X \rightarrow \mu^+\mu^-} = \frac{Y^2}{8\pi} M_X \left(1 - \frac{4m_\mu^2}{M_X^2}\right)^{3/2} = (1.8 \pm 0.5) \text{ MeV}, \quad (2)$$

while according to [16] the width of the peak is

$$\Gamma_X^{\text{exp}} = (1.8 \pm 0.8) \text{ GeV}, \quad (3)$$

which is only several times bigger than the detector mass resolution for a dimuon system $\sigma = 0.45 \text{ GeV}$. That is why we will also consider the case of Γ_X approximately equal to $\Gamma_{X \rightarrow \mu^+ \mu^-}$ given in (2).

2 The fiducial cross section of the $pp(\gamma\gamma) \rightarrow pp\mu^+\mu^-$ reaction

We are interested in the contribution of the X resonance to this cross section. In [15] the cross section of $\mu^+\mu^-$ production was measured in four intervals of muon pair invariant mass on which the entire interval $12 \text{ GeV} < m_{\mu^+\mu^-} < 70 \text{ GeV}$ was divided. We are interested in the interval $22 \text{ GeV} < m_{\mu^+\mu^-} < 30 \text{ GeV}$, for which, according to Table 3 of [15],

$$\frac{d\sigma^{\text{exp}}}{dm_{\mu^+\mu^-}} = (0.076 \pm 0.005) \frac{\text{pb}}{\text{GeV}}, \quad \text{hence} \quad \sigma^{\text{exp}} = (0.61 \pm 0.04) \text{ pb}. \quad (4)$$

This cross section measurement corresponds to the fiducial region $p_T^\mu > \hat{p}_T = 6 \text{ GeV}$ and $|\eta| < \hat{\eta}_T = 2.4$, where p_T^μ is the component of the muon momentum transversal to the proton beam and η is the muon pseudorapidity: $\eta = -\ln \tan(\theta/2)$, where θ is the angle between the muon momentum and the beam. The ATLAS muon spectrometer is measuring muon momentum up to $|\eta| = 2.7$, but the trigger chambers cover the range $|\eta| < 2.4$ that corresponds to the pseudorapidity cutoff given above.

According to the equivalent photons approximation the cross section of $\mu^+\mu^-$ pair production in ultraperipheral collisions is given by:

$$\sigma(pp(\gamma\gamma) \rightarrow pp\mu^+\mu^-) = \int_0^\infty d\omega_1 \int_0^\infty d\omega_2 \sigma(\gamma\gamma \rightarrow \mu^+\mu^-) n(\omega_1) n(\omega_2), \quad (5)$$

where $n(\omega)$ is the equivalent photons spectrum. In the leading logarithmic approximation (LL)

$$n(\omega) \approx n_{\text{LL}}(\omega) = \frac{2\alpha}{\pi\omega} \ln \frac{\hat{q}\gamma}{\omega}, \quad (6)$$

where α is the fine structure constant, $\gamma = 6.93 \times 10^3$ is the Lorentz factor of the proton with the energy 6.5 TeV, and \hat{q} is the maximal photon momentum at which the proton does not disintegrate. In this approximation the integrals in Eq. (5) are divergent, and the integration domain is cut off explicitly with $\hat{q}\gamma$:

$$\sigma_{\text{LL}}(pp(\gamma\gamma) \rightarrow pp\mu^+\mu^-) = \int_{m_\mu^2/\hat{q}\gamma}^{\hat{q}\gamma} d\omega_1 \int_{m_\mu^2/\omega_1}^{\hat{q}\gamma} d\omega_2 \sigma(\gamma\gamma \rightarrow \mu^+\mu^-) n_{\text{LL}}(\omega_1) n_{\text{LL}}(\omega_2), \quad (7)$$

The value of \hat{q} is determined by the proton form factor and numerically $\hat{q} \approx 0.20 \text{ GeV}$ [18].

It is convenient to substitute the integration over photon energies by integration over $s = 4\omega_1\omega_2$ and $x = \omega_1/\omega_2$. Then Eq. (5) changes to

$$\sigma(pp(\gamma\gamma) \rightarrow pp\mu^+\mu^-) = \int_{(2m_\mu)^2}^\infty \sigma(\gamma\gamma \rightarrow \mu^+\mu^-) ds \int_0^\infty \frac{dx}{8x} n\left(\sqrt{\frac{sx}{4}}\right) n\left(\sqrt{\frac{s}{4x}}\right). \quad (8)$$

To take the experimental cuts into account, we substitute $\sigma(\gamma\gamma \rightarrow \mu^+\mu^-)$ by the differential over p_T cross section:

$$\sigma(pp(\gamma\gamma) \rightarrow pp\mu^+\mu^-) = \int_{(2m_\mu)^2}^\infty ds \int_0^{\sqrt{s}/2} \frac{d\sigma(\gamma\gamma \rightarrow \mu^+\mu^-)}{dp_T} dp_T \int_0^\infty \frac{dx}{8x} n\left(\sqrt{\frac{sx}{4}}\right) n\left(\sqrt{\frac{s}{4x}}\right). \quad (9)$$

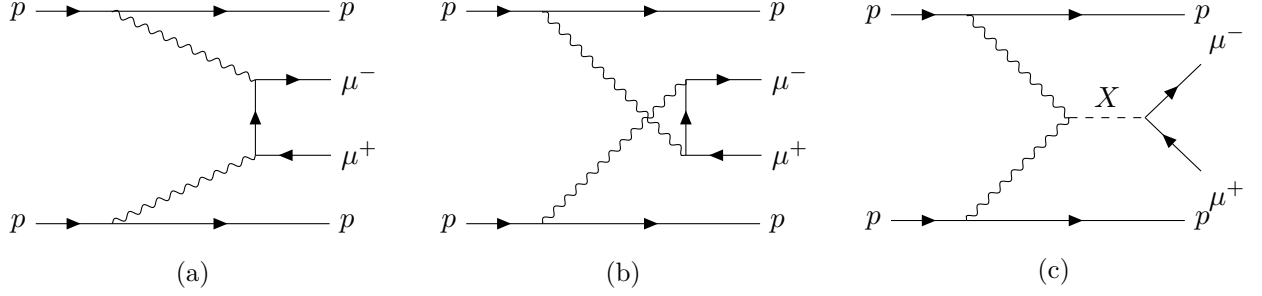


Figure 1: Diagrams which contribute to the production of muon pair in ultraperipheral pp collisions

It is then straightforward to implement cuts over s and p_T by changing the integration limits to $\hat{s}_{\min} < s < \hat{s}_{\max}$ and $\hat{p}_T < p_T < \sqrt{s}/2$ (assuming $\hat{s}_{\min} \geq (2\hat{p}_T)^2 \gg (2m_\mu)^2$). To implement the cutoff over pseudorapidity, one should integrate over x in the interval [18]

$$\frac{1}{\hat{x}} < x < \hat{x}, \quad \text{where } \hat{x} = \exp(2\hat{\eta}) \frac{1 - \sqrt{1 - 4p_T^2/s}}{1 + \sqrt{1 - 4p_T^2/s}}. \quad (10)$$

Let us note that in the leading logarithmic approximation from the condition $\omega \lesssim \hat{q}\gamma$ it follows that x should be always smaller than $(2\hat{q}\gamma/\sqrt{s})^2$. For numerical values of $\hat{\eta}$, \hat{p}_T and $\hat{s} = \{\hat{s}_{\min}, \hat{s}_{\max}\}$ we are interested in and for x from the interval (10) this demand is satisfied.

Thus for the fiducial cross section we obtain:

$$\sigma_{\text{fid}}^{\hat{s}, \hat{p}_T, \hat{\eta}} = \int_{\hat{s}_{\min}}^{\hat{s}_{\max}} ds \int_{\hat{p}_T}^{\sqrt{s}/2} \frac{d\sigma(\gamma\gamma \rightarrow \mu^+ \mu^-)}{dp_T} dp_T \int_{1/\hat{x}}^{\hat{x}} \frac{dx}{8x} n\left(\sqrt{\frac{s}{4}}\right) n\left(\sqrt{\frac{s}{4x}}\right), \quad (11)$$

where \hat{x} is defined in (10). In the leading logarithmic approximation the fiducial cross section is

$$\sigma_{\text{fid,LL}}^{\hat{s}, \hat{p}_T, \hat{\eta}} = \frac{\alpha^2}{\pi^2} \int_{\hat{s}_{\min}}^{\hat{s}_{\max}} \ln^2 \frac{(2\hat{q}\gamma)^2}{s} \frac{ds}{s} \int_{\hat{p}_T}^{\sqrt{s}/2} \frac{d\sigma(\gamma\gamma \rightarrow \mu^+ \mu^-)}{dp_T} \left[1 - \frac{1}{3} \left(\frac{\ln \hat{x}}{\ln \frac{(2\hat{q}\gamma)^2}{s}} \right)^2 \right] \ln \hat{x} dp_T. \quad (12)$$

Let us begin with the calculation of the Standard Model contribution to the cross section of $\mu^+ \mu^-$ pair production, given by the diagrams shown in Figs. 1a, 1b.

The expression for the differential cross section is [19, §88]:

$$d\sigma(\gamma\gamma \rightarrow \mu^+ \mu^-) = \frac{2\pi\alpha^2}{s^2} \left(\frac{s+t}{t} + \frac{t}{s+t} \right) dt = \frac{8\pi\alpha^2}{s p_T} \frac{1 - 2p_T^2/s}{\sqrt{1 - 4p_T^2/s}} dp_T. \quad (13)$$

Substituting it in (12) and integrating over p_T we get:

$$\sigma_{\text{fid,LL}}^{\hat{s}, \hat{p}_T, \hat{\eta}} \approx \frac{8\alpha^4}{\pi} \int_{\hat{s}_{\min}}^{\hat{s}_{\max}} \ln^2 \frac{(2\hat{q}\gamma)^2}{s} \frac{ds}{s^2} \left\{ \hat{\eta} \left[\ln \left(\frac{1 + \sqrt{1 + 4\hat{p}_T^2/s}}{1 - \sqrt{1 - 4\hat{p}_T^2/s}} \right) - \sqrt{1 - \frac{4\hat{p}_T^2}{s}} \right] - \right. \\ \left. - \frac{1}{4} \ln^2 \left(\frac{1 + \sqrt{1 + 4\hat{p}_T^2/s}}{1 - \sqrt{1 - 4\hat{p}_T^2/s}} \right) + \frac{1}{2} \sqrt{1 - \frac{4\hat{p}_T^2}{s}} \ln \left(\frac{1 + \sqrt{1 + 4\hat{p}_T^2/s}}{1 - \sqrt{1 - 4\hat{p}_T^2/s}} \right) \right\} = 0.73 \text{ pb}, \quad (14)$$

where we neglected the small second term in the square brackets in (12) in order to perform integration analytically. Taking into account the omitted term and integrating numerically in (12), instead of 0.73 pb we obtain 0.68 pb.

More accurate calculation depends on the internal structure of proton and the probability for the protons to survive the collision. The latter is [20]

$$P(b) = \left(1 - e^{-\frac{b^2}{2B}}\right)^2, \quad (15)$$

where b is the impact parameter of the collision, and B was measured to be 19.7 GeV^{-2} in the case of pp collisions with the energy 7 TeV [21]. To utilize this function we introduce the equivalent photon spectrum at the distance b from the source particle $n(b, \omega)$ such that

$$n(\omega) = \int n(b, \omega) d^2 b. \quad (16)$$

Then the leading logarithmic spectrum [22, §15.5]

$$n_{\text{LL}}(b, \omega) = \frac{\alpha \omega}{\pi^2 \gamma^2} K_1 \left(\frac{b \omega}{\gamma} \right), \quad (17)$$

where K_1 is the modified Bessel function of the second kind (the Macdonald function).

In this framework Eq. (5) is replaced with

$$\begin{aligned} \sigma(pp(\gamma\gamma) \rightarrow pp\mu^+\mu^-) = \int_0^\infty d\omega_1 \int_0^\infty d\omega_2 \sigma(\gamma\gamma \rightarrow \mu^+\mu^-) \times \\ \times \int d^2 b_1 \int d^2 b_2 n(b_1, \omega_1) n(b_2, \omega_2) P(|\mathbf{b}_1 - \mathbf{b}_2|). \end{aligned} \quad (18)$$

This change is then propagated into Eq. (11):

$$\begin{aligned} \sigma_{\text{fid}}^{\hat{s}, \hat{p}_T, \hat{\eta}} = \int_{\hat{s}_{\text{min}}}^{\hat{s}_{\text{max}}} ds \int_{\hat{p}_T}^{\sqrt{s}/2} dp_T \frac{d\sigma(\gamma\gamma \rightarrow \mu^+\mu^-)}{dp_T} \times \\ \times \int_{1/\hat{x}}^{\hat{x}} \frac{dx}{8x} \int_{b_1 > 0} d^2 b_1 \int_{b_2 > 0} d^2 b_2 n\left(b_1, \sqrt{\frac{sx}{4}}\right) n\left(b_2, \sqrt{\frac{s}{4x}}\right) P(|\mathbf{b}_1 - \mathbf{b}_2|). \end{aligned} \quad (19)$$

The internal structure of proton is characterized by the Dirac form factor [23]

$$F_1(Q^2) = G_D(Q^2) \left[1 + \frac{(\mu_p - 1)\tau}{1 + \tau} \right], \quad G_D(Q^2) = \frac{1}{(1 + \frac{Q^2}{\Lambda^2})^2}, \quad (20)$$

where $Q^2 = -q^2$, q is the photon 4-momentum, $\tau = Q^2/4m_p^2$, m_p is the proton mass and $\mu_p = 2.7928473508(85)$ is the proton magnetic moment [24], $G_D(Q^2)$ is the dipole form factor with Λ being strictly fixed by the proton charge radius: $\Lambda^2 = 12/r_p^2$, $r_p = 0.8751(61) \text{ fm}$ [24].

The form factor enters Eqs. (5), (19) through the equivalent photon spectrum [18]:

$$n(\omega) = \frac{\alpha}{\pi^2 \omega} \int \frac{\vec{q}_\perp^2 F_1^2(\vec{q}_\perp^2 + \omega^2/\gamma^2)}{(\vec{q}_\perp^2 + \omega^2/\gamma^2)^2} d^2 q_\perp, \quad (21)$$

$$n(b, \omega) = \frac{\alpha}{\pi^2 \omega} \left[\int d q_\perp q_\perp^2 \frac{F_1(q_\perp^2 + \omega^2/\gamma^2)}{q_\perp^2 + \omega^2/\gamma^2} J_1(b q_\perp) \right]^2, \quad (22)$$

where J_1 is the Bessel function of the first kind.

Table 1: The measured cross section for each interval of muon pair invariant mass and the corresponding theoretical calculations with different approximations: Eq.(12) is the calculation with the equivalent photon spectrum taken in the leading logarithmic approximation; Eqs.(11), (21) is the calculation taking into account the proton electromagnetic form factor; Eq.(19), (22) also accounts for the probability of strong interactions at small impact parameters. "Survival ratio" is the ratio of the preceding two columns. Note that for the interval $30 - 70$ GeV the cutoff $\hat{p}_T = 10$ GeV as it is in [15].

$m_{\mu^+\mu^-}$, GeV	σ^{exp} , pb	$\sigma_{\text{fid,LL}}^{\hat{s},\hat{p}_T,\hat{\eta}}$, pb, Eq. (12)	$\sigma_{\text{fid}}^{\hat{s},\hat{p}_T,\hat{\eta}}$, pb, Eqs. (11), (21)	$\sigma_{\text{fid}}^{\hat{s},\hat{p}_T,\hat{\eta}}$, pb, Eqs. (19), (22)	Survival ratio
12 – 17	1.22 ± 0.07	1.25	1.28	1.24	0.970
17 – 22	0.82 ± 0.05	0.87	0.896	0.866	0.967
22 – 30	0.61 ± 0.04	0.68	0.703	0.677	0.963
30 – 70	0.52 ± 0.04	0.49	0.506	0.483	0.953

The so-called survival factor $S_{\gamma\gamma}^2$ [18,20,25] is defined as the ratio of the integrands in Eqs. (5), (18):¹

$$S_{\gamma\gamma}^2 = \frac{\int_{b_1 > 0} \int_{b_2 > 0} n(b_1, \omega_1) n(b_2, \omega_2) P(|\mathbf{b}_1 - \mathbf{b}_2|) d^2 b_1 d^2 b_2}{n(\omega_1) n(\omega_2)}, \quad (23)$$

however in this paper it is not calculated explicitly; Eq. (19) is used instead.

Calculations for each interval of muon pair invariant mass for Eq. (12), Eq. (11) with the spectrum (21), and Eq. (19) with the spectrum (22) are presented in the Table 1. One can see that accounting for inelastic pp scattering reduces the theoretical result by 5% approximately.

The amplitude of the $\mu^+\mu^-$ pair production through intermediate X boson in $\gamma\gamma$ collisions (see Fig. 1c) is given by the following expression

$$A = \kappa F_{\mu\nu}^1 F_{\mu\nu}^2 \frac{1}{s - M_X^2 + i\Gamma_X M_X} \bar{\mu}\mu Y, \quad (24)$$

where κ is the $X\gamma\gamma$ coupling constant so that $\Gamma_{X\rightarrow\gamma\gamma} = (\kappa^2 M_X^3)/(16\pi)$. For the cross section of the $\gamma\gamma \rightarrow X \rightarrow \mu^+\mu^-$ reaction we obtain:

$$|A|^2 = \kappa^2 Y^2 M_X^6 \frac{1}{(s - M_X^2)^2 + \Gamma_X^2 M_X^2}, \quad (25)$$

$$\sigma_{\gamma\gamma \rightarrow X \rightarrow \mu^+\mu^-} = \frac{2\pi}{M_X^2} \frac{\Gamma_{X\rightarrow\gamma\gamma} \Gamma_{X\rightarrow\mu^+\mu^-}}{(\sqrt{s} - M_X)^2 + \Gamma_X^2/4}, \quad (26)$$

where the factor 2 takes into account identity of photons.

In the limit $m_\mu \rightarrow 0$ chiralities of the muons produced through the diagrams in Figs. 1a, 1b are not the same as in Fig. 1c. Consequently, these diagrams do not interfere in this limit. Even with nonzero m_μ the interference is zero at $s = M_X^2$ because then the phase between the sum of the diagrams in Figs. 1a, 1b and the diagram in Fig. 1c is $\pi/2$. For other values of s the interference is suppressed relatively to X contribution by the factor $\frac{\alpha\Gamma_X}{\sqrt{\Gamma_{X\rightarrow\mu^+\mu^-} - \Gamma_{X\rightarrow\gamma\gamma}}} \frac{m_\mu}{M_X} \left(1 - \frac{M_X^2}{s}\right)$ which is less than 10^{-2} for the largest allowed values of $\Gamma_{X\rightarrow\gamma\gamma}$ in both cases of the narrow or the wide resonance ($\Gamma_X = 1.8$ MeV or 1.8 GeV respectively).

¹Survival factor can be also defined in a more elaborate way: on the amplitude level. See [26–32] for details.

Let us also note that definition of $S_{\gamma\gamma}^2$ in Ref. [33] (Eq. (7)) is different: Ref. [33] requires that the new system is produced outside of the colliding particles, while Ref. [18] imposes no such restriction. The latter is more accurate when the new particles do not interact strongly, so we use the Ref. [18] definition of $S_{\gamma\gamma}^2$ here. In paper [32] it was specifically stressed that impact parameter cut like in Ref. [33] is unphysical.

In order to impose the cut on the transverse momentum of muons with the help of expression (11) the following differential cross section is used:

$$d\sigma = \frac{|A|^2}{32\pi s} \frac{d(4p_T^2/s)}{\sqrt{1-4p_T^2/s}}. \quad (27)$$

Substituting (27) and (25) in (12) and performing integration over p_T we obtain:

$$\begin{aligned} \sigma_{\text{fid,LL}}^{\hat{s},\hat{p}_T,\hat{\eta}}(X) = & \frac{8\alpha^2\Gamma_{X\rightarrow\gamma\gamma}\Gamma_{X\rightarrow\mu^+\mu^-}}{\pi M_X^2} \int_{\hat{s}_{\min}}^{\hat{s}_{\max}} \frac{ds}{(s-M_X^2)^2 + \Gamma_X^2 M_X^2} \ln^2 \frac{(2\hat{q}\gamma)^2}{s} \times \\ & \times \left[\sqrt{1 - \frac{4\hat{p}_T^2}{s}} \left(2\hat{\eta} + \ln \left(\frac{1 - \sqrt{1 - 4\hat{p}_T^2/s}}{1 + \sqrt{1 - 4\hat{p}_T^2/s}} \right) \right) - \ln \frac{4\hat{p}_T^2}{s} \right]. \end{aligned} \quad (28)$$

In the case of narrow resonance $\Gamma_X \approx \Gamma_{X\rightarrow\mu^+\mu^-} = (1.8 \pm 0.5) \text{ MeV}$ the integration can be performed analytically and we obtain:

$$\begin{aligned} \sigma_{\text{fid,LL}}^{\hat{s},\hat{p}_T,\hat{\eta}}(X) = & \frac{8\alpha^2\Gamma_{X\rightarrow\gamma\gamma}\Gamma_{X\rightarrow\mu^+\mu^-}}{\Gamma_X M_X^3} \ln^2 \frac{(2\hat{q}\gamma)^2}{M_X^2} \times \\ & \times \left[\sqrt{1 - \frac{4\hat{p}_T^2}{M_X^2}} \left(2\hat{\eta} + \ln \left(\frac{1 - \sqrt{1 - 4\hat{p}_T^2/M_X^2}}{1 + \sqrt{1 - 4\hat{p}_T^2/M_X^2}} \right) \right) - \ln \frac{4\hat{p}_T^2}{M_X^2} \right] \approx \\ & \approx 6.1 \times 10^4 \frac{\Gamma_{X\rightarrow\mu^+\mu^-}}{M_X} \frac{\Gamma_{X\rightarrow\gamma\gamma}}{\Gamma_X} \text{ pb}. \end{aligned} \quad (29)$$

However if $\Gamma_X = (1.8 \pm 0.8) \text{ GeV}$ then the width of the resonance almost equals $\sqrt{\hat{s}_{\max}} - M_X = 2 \text{ GeV}$ so the integration should be done numerically and we obtain:

$$\sigma_{\text{fid,LL}}^{\hat{s},\hat{p}_T,\hat{\eta}}(X) \approx 49 \frac{\Gamma_{X\rightarrow\gamma\gamma}}{M_X} \text{ pb}. \quad (30)$$

3 Numerical estimates

From the third line of the second and the fifth columns of the Table we see that the contribution of the resonance X into the fiducial cross section of muon pair production is bounded in the following way:²

$$\sigma_{\text{fid}}(X) \lesssim 0.10 \text{ pb at 99.5\% confidence level}. \quad (31)$$

Comparing this number with the expression (29) we get that if $\Gamma_X \approx \Gamma_{X\rightarrow\mu^+\mu^-}$ then the upper bound on $\Gamma_{X\rightarrow\gamma\gamma}$ is:

$$\text{Br}(X \rightarrow \gamma\gamma) < 2.6 \times 10^{-2}, \Gamma_{X\rightarrow\gamma\gamma} < 46 \text{ keV} \approx 1.6 \times 10^{-6} M_X \text{ at 99.5\% confidence level} (\Gamma_X = 1.8 \text{ MeV}). \quad (32)$$

If the width of X is given by (3) then the bound extracted from Eq.(30) is:

$$\text{Br}(X \rightarrow \gamma\gamma) < 3.2 \times 10^{-2}, \Gamma_{X\rightarrow\gamma\gamma} < 58 \text{ MeV} \approx 2 \times 10^{-3} M_X \text{ at 99.5\% confidence level} (\Gamma_X = 1.8 \text{ GeV}). \quad (33)$$

Resonance X couples with photons through a triangle diagram with fermion running in the loop (see Fig. 2). Let us check that the corresponding decay probability does not violate bounds just obtained.

²This upper limit was calculated according to the recommendation in [34], neglecting the theoretical error on the estimated background.

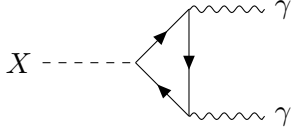


Figure 2: Coupling of X to two photons through a fermion loop

The amplitude generated by the triangle diagram with a fermion f running in the loop equals [35]:

$$A = \frac{\alpha F}{4\pi} Y_{Xff} \frac{1}{m_f} X F_{\mu\nu}^1 F_{\mu\nu}^2. \quad (34)$$

The width equals:

$$\Gamma_{X \rightarrow \gamma\gamma} = \frac{\alpha^2 F^2}{256\pi^3} Y_{Xff}^2 \left(\frac{M_X}{m_f} \right)^2 M_X, \quad (35)$$

where

$$F = -2\beta[(1-\beta)\varkappa^2 + 1], \quad \beta = \frac{4m_f^2}{M_X^2}, \quad (36)$$

$$\varkappa = \begin{cases} \arctan\left(\frac{1}{\sqrt{\beta-1}}\right), & \beta > 1 \\ \frac{1}{2}\left[i \ln\left(\frac{1+\sqrt{1-\beta}}{1-\sqrt{1-\beta}}\right) + \pi\right], & \beta < 1. \end{cases} \quad (37)$$

For $m_f \ll M_X$ we obtain $F \sim (m_f/M_X)^2$ and for $m_f \gg M_X$ we obtain $F \rightarrow -4/3$.

In the case of muon running in the loop we get $\Gamma_{X \rightarrow \gamma\gamma} \approx 10^{-11} M_X$ which is much smaller than bounds (32), (33). For a hypothetical fermion with mass much larger than M_X the width is also very small. However for $m_f \sim M_X$ and $Y_{Xff} \sim 1$ it approaches keV: $\Gamma_{X \rightarrow \gamma\gamma}(m_f = M_X/2) \approx 3Y_{Xff}^2$ keV.

4 Conclusions

A scalar resonance with the mass 28 GeV coupling to muons in the way consistent with the recent CMS data [16] is also consistent with the measurements of the cross section for muon pair production in ultraperipheral collisions at the LHC [15] provided that the width of its decay to a pair of photons $\Gamma_{X \rightarrow \gamma\gamma} < 46$ keV or 58 MeV depending on whether the width $\Gamma_X = 1.8$ GeV reported in Ref. [16] is the real width of the resonance or an artifact of the detector mass resolution.

The difference between the leading logarithmic approximation and the calculation that takes into account both the proton form factor and the survival factor for the protons colliding with the energy 13 TeV is at the level of few percent. Integration of the logarithmic approximation can often be performed analytically while the form factor and especially the survival factor require computationally expensive numerical calculations. Therefore cross sections for ultraperipheral collisions of protons in the lower region of invariant masses of the produced system can be estimated in the logarithmic approximation with the form factor and the survival factor taken into account as needed.

Our study demonstrates that we can look for New Physics in ultraperipheral collisions at the LHC.

We are grateful to V.B. Gavrilov and A.N. Nikitenko, who have brought the CMS observation of $X(28\text{GeV})$ to our attention. We are grateful to V.A. Khoze for drawing our attention to papers [26–32]. We are supported by the Russian Science Foundation grant No 19-12-00123.

References

[1] CMS Collaboration, *Exclusive photon-photon production of muon pairs in proton-proton collisions at $\sqrt{s} = 7$ TeV*, JHEP **01** (2012) 052; arXiv:1111.5536 [hep-ex].

[2] ATLAS Collaboration, *Measurement of exclusive $\gamma\gamma \rightarrow l^+l^-$ production in proton-proton collisions at $\sqrt{s} = 7$ TeV with the ATLAS detector*, Phys. Lett. B **749** (2015) 242; arXiv:1506.07098 [hep-ex].

[3] CMS Collaboration, *Search for exclusive or semi-exclusive photon pair production and observation of exclusive and semi-exclusive electron pair production in pp collisions at $\sqrt{s} = 7$ TeV*, JHEP **11** (2012) 080; arXiv:1209.1666 [hep-ex].

[4] CMS Collaboration, *Study of exclusive two-photon production of W^+W^- in pp collisions at $\sqrt{s} = 7$ TeV and constraints on anomalous quartic gauge couplings*, JHEP **07** (2013) 116; arXiv:1305.5596 [hep-ex].

[5] CMS Collaboration, *Evidence for exclusive $\gamma\gamma \rightarrow W^+W^-$ production and constraints on anomalous quartic gauge couplings in pp collisions at $\sqrt{s} = 7$ and 8 TeV*, JHEP **08** (2016) 119; arXiv:1604.04464 [hep-ex].

[6] ATLAS Collaboration, *Measurement of exclusive $\gamma\gamma \rightarrow W^+W^-$ production and search for exclusive Higgs boson production in pp collisions at $\sqrt{s} = 8$ TeV using the ATLAS detector*, Phys. Rev. D **94** (2016) 032011; arXiv:1607.03745 [hep-ex].

[7] ATLAS Collaboration, *Observation of photon-induced W^+W^- production in pp collisions at $\sqrt{s} = 13$ TeV using the ATLAS detector*, CERN-EP-2020-165 (2020); arXiv:2010.04019 [hep-ex].

[8] ATLAS Collaboration, *Evidence for light-by-light scattering in heavy-ion collisions with the ATLAS detector at the LHC*, Nat. Phys. **13** (2017) 852; arXiv:1702.01625 [hep-ex].

[9] CMS Collaboration, *Evidence for light-by-light scattering in ultraperipheral PbPb collisions at $\sqrt{s_{NN}} = 5.02$ TeV*, Nucl. Phys. A **982** (2019) 791 ; arXiv:1808.03524 [hep-ex].

[10] ATLAS Collaboration, *Observation of light-by-light scattering in ultraperipheral Pb+Pb collisions with the ATLAS detector*, Phys. Rev. Lett. **123** (2019) 052001; arXiv:1904.03536 [hep-ex].

[11] Godunov S I, Novikov V A, Rozanov A N, Vysotsky M I, Zhemchugov E V, *Quasistable charginos in ultraperipheral proton-proton collisions at the LHC*, JHEP **01** (2020) 143; arXiv: 1906.08568 [hep-ph].

[12] Harland-Lang L A, Khoze V A, Ryskin M G, Tasevsky M, *LHC Searches for Dark Matter in Compressed Mass Scenarios: Challenges in the Forward Proton Mode* , JHEP **04** (2019) 010; arXiv:1812.04886 [hep-ph].

[13] Khoze V A, Martin A D, Ryskin M G, *Can invisible objects be ‘seen’ via forward proton detectors at the LHC?*, J. Phys. G: Nucl. Part. Phys. **44** (2017) 055002; arXiv:1702.05023 [hep-ph].

[14] Tasevsky M, Harland-Lang L A, Khoze V A, Ryskin M G, *Searches for Dark Matter at the LHC in forward proton mode*, EPS-HEP2019 (2019); arXiv:1910.01703 [hep-ph].

[15] ATLAS Collaboration, *Measurement of the exclusive $\gamma\gamma \rightarrow \mu^+\mu^-$ process in proton-proton collisions at $\sqrt{s} = 13$ TeV with the ATLAS detector*, Phys. Lett. B **777** (2018) 303; arXiv:1708.04053 [hep-ex].

[16] CMS Collaboration, *Search for resonances in the mass spectrum of muon pairs produced in association with b quark jets in proton-proton collisions at $\sqrt{s} = 8$ and 13 TeV*, JHEP **11** (2018) 161; arXiv:1808.01890 [hep-ex].

[17] Godunov S I, Novikov V A, Vysotsky M I, Zhemchugov E V, *Dimuon resonance near 28 GeV and muon anomaly*, JETP Lett. **109** (2019) 358; arXiv:1808.02431 [hep-ph].

[18] Vysotsky M I, Zhemchugov E V, *Equivalent photons in proton-proton and ion-ion collisions at the LHC*, Phys. Usp. **62** (2019) 910–919; Translated from Russian: UFN, **189** (2019) 975; arXiv:1806.07238 [hep-ph].

[19] Berestetskii V B, Lifshitz E M, Pitaevskii L P *Quantum Electrodynamics* (Oxford: Pergamon Press, 1982); Translated from Russian: *Kvantovaya Elektrodinamika* (Moscow: Nauka, 1989).

[20] Frankfurt L, Hyde-Wright C E, Strikman M, Weiss C, *Generalized parton distributions and rapidity gap survival in exclusive diffractive pp scattering*, Phys. Rev. D **75** (2007) 054009; arXiv:0608271 [hep-ph].

[21] ATLAS Collaboration, *Measurement of the total cross section from elastic scattering in pp collisions at $\sqrt{s} = 7\text{TeV}$ with the ATLAS detector*, Nucl. Phys. B **889** (2014) 486; arXiv:1408.5778 [hep-ex].

[22] Jackson J D, *Classical Electrodynamics* (New York City: John Wiley & Sons, 1962).

[23] Pacetti S, Ferroli R B, Tomasi-Gustafsson E *Proton electromagnetic form factors: Basic notions, present achievements and future perspectives*, Phys. Rep. **550 – 551** (2015) 1.

[24] Mohr P J, Newell D B and Taylor B N, *CODATA Recommended Values of the Fundamental Physical Constants: 2014*, Rev. Mod. Phys. **88** (2016) 035009; arXiv:1507.07956 [physics.atom-ph].

[25] Godunov S I, Novikov V A, Rozanov A N, Vysotsky M I, Zhemchugov E V, paper in preparation.

[26] Khoze V A, Martin A D, Orava R and Ryskin M G, *Luminosity monitors at the LHC*, Eur. Phys. J. C **19** (2001), 313-322; arXiv:hep-ph/0010163 [hep-ph].

[27] Khoze V A, Martin A D and Ryskin M G, *Photon exchange processes at hadron colliders as a probe of the dynamics of diffraction*, Eur. Phys. J. C **24** (2002), 459-468; arXiv:hep-ph/0201301 [hep-ph].

[28] Khoze V A, Martin A D and Ryskin M G, *Elastic scattering and Diffractive dissociation in the light of LHC data*, Int. J. Mod. Phys. A **30** (2015) no.08, 1542004; arXiv:1402.2778 [hep-ph].

[29] Harland-Lang L A, Khoze V A, Ryskin M G and Stirling W J, *Central exclusive production within the Durham model: a review*, Int. J. Mod. Phys. A **29** (2014), 1430031; arXiv:1405.0018 [hep-ph].

[30] Harland-Lang L A, Khoze V A and Ryskin M G, *Exclusive physics at the LHC with SuperChic 2*, Eur. Phys. J. C **76** (2016) no.1, 9; arXiv:1508.02718 [hep-ph].

[31] Khoze V A, Martin A D and Ryskin M G, *Multiple interactions and rapidity gap survival*, J. Phys. G **45** (2018) no.5, 053002; arXiv:1710.11505 [hep-ph].

[32] Harland-Lang L A, Tasevsky M, Khoze V A and Ryskin M G, *A new approach to modelling elastic and inelastic photon-initiated production at the LHC: SuperChic 4*, Eur. Phys. J. C **80** (2020) no.10, 925; arXiv:2007.12704 [hep-ph].

[33] Dyndal M, Schoeffel L, *The role of finite-size effects on the spectrum of equivalent photons in proton-proton collisions at the LHC*, Phys. Lett. B **741** (2015) 66; arXiv:1410.2983 [hep-ph].

[34] Cowan G, Cranmer K, Gross E and Vitells O, *Asymptotic formulae for likelihood-based tests of new physics*, Eur. Phys. J. C **71** (2011) 1554 [erratum: Eur. Phys. J. C **73** (2013) 2501]; arXiv:1007.1727 [physics.data-an].

[35] Shifman M A, Vainshtein A I, Voloshin M B, Zakharov V I, *Low-energy theorems for Higgs boson couplings to photons*, Sov. J. Nucl. Phys. **30** (1979) 711-716.